Solar Energy Vol. 35, No. 2, pp. 189–197, 1985
Printed in the U.S.A.

0038–092X/85 $3.00 + .00
Pergamon Press Ltd.

TECHNICAL NOTE

A design method for active–passive hybrid space heating systems

B. L. EVANS, S. A. KLEIN and J. A. DUFFIE
Solar Energy Laboratory, University of Wisconsin-Madison, 1500 Johnson Drive, Madison, WI 53706

(*Received* 31 *May* 1984; *accepted* 27 *December* 1984)

1. INTRODUCTION

The combination of active and passive solar space heating systems is attractive due to the complimentary nature of the two system types. Passive systems are typically less expensive and simpler than active systems, yet in many climates, it is difficult to meet a high fraction of the heating requirements with passive heating alone because of the need for large glazing areas and the difficulty in efficiently storing energy in the building structure for extended periods. Active solar systems provide additional energy input and can more efficiently store energy for later use. Combining these systems provides the efficient storage capacity of the active system and allows a reduction in active system size, hence cost, compared to an active-only system because the passive system meets a portion of the heating load.

Almost all active systems can be considered active–passive hybrid systems since any windows which contribute a net solar gain can be considered to be a passive solar system. Although hybrid systems have great potential, there has been no generalized design method available to analyze their performance. The objective of this paper is to present a design method for hybrid systems through the combination of existing design methods for active and passive systems.

2. PROBLEMS ASSOCIATED WITH COMBINING DESIGN METHODS

A possible procedure for analyzing a hybrid system is to first apply a passive design method (e.g., the Solar-Load Ratio[7, 13], or Un-utilizability[8, 9] methods), assuming that there is no active system. The additional energy needed to maintain the building above its set point is predicted by the passive design method and then is used as the heating load for the active system. The result of the active system design method (e.g. the f-Chart method[2]) is then the estimate of the auxiliary which must be supplied for the combined active–passive system. This infers that the passive system has the first opportunity to supply energy for the heating load, and the active system is essentially a backup, as it is more controllable than the passive system.

There are two problems with this approach to hybrid system analysis. First, the load on the active system will always be greater than the auxiliary energy predicted by the passive system design method (disregarding systematic or location dependent errors in the design method) because the active system controller causes the average building temperature to be greater than it would be if the active solar system were not present.

The second problem is concerned with the time distribution of the load on the active system. Active system design methods such as f-Chart[2] assume that the space heating load is proportional to the difference between the indoor and outdoor temperature. In a hybrid system, the passive component will supply much of the load during the day, shifting the load distribution for the active system to nighttime periods. These two problems can be accounted for by use of two corrections that are part of the design method given in this paper.

3. IDENTIFICATION OF IMPORTANT PARAMETERS

In order to investigate which system components and parameters are important in causing the interaction between active and passive components in hybrid systems, a series of TRNSYS[1] simulations were run in which timed artificial "passive gains" were input into the building model. The distribution and intensity of the artificial passive gains were controlled in a manner which allowed the effect of changes in parameters and components on active system performance to be readily apparent.

In addition to the artificial "passive" energy gain parameters, a number of building and active solar system parameters were also investigated. Of these, four were found to cause interactions between the active and passive system performance. These are: active system collector size relative to the building energy losses not met by passive; active system storage capacity per unit collector area; active system load heat exchanger size; and effective building energy storage capacity.

Using controlled "passive gains" allowed inexpensive screening to select parameters for further study using detailed passive models on an annual basis. In the subsequent detailed studies, standard components of the TRNSYS 11.1 simulation program are used for both the active and passive systems.

4. MAGNITUDE CORRECTION FOR ACTIVE SYSTEM LOAD

The error in the passive design method prediction of the magnitude of the active system load is primarily a function of the active system controller. The increase in load on the active system above that predicted by the passive system design method results from the active solar thermostat set temperature being higher than the auxiliary system thermostat set temperature. A higher set temperature is necessary to ensure that available solar energy is used before auxiliary energy is supplied. Higher active solar fractions mean that the building is at the higher set temperature more often, causing the average building temperature to be higher. Higher building temperatures will result in additional energy losses from the building, hence more load on the system.

A monthly energy balance on a hybrid system leads to a generalized correction factor for L/L_o, the ratio of the active system load, L, to the active system load as predicted by the passive design method, L_o. The correction factor is in terms of the monthly passive solar fraction, f_p, defined in eqn (1); the monthly active solar fraction, f_a, defined in eqn (2); the monthly heating degree days, DD (based on the building base temperature); the building shell energy loss coefficient (not including the passive collector) UA_b; and the passive collector energy loss coefficient, UA_c.

$$f_p = 1 - \frac{L_o}{UA_b(DD)}, \quad (1)$$

$$f_a = 1 - \frac{Q_{aux}}{L}. \quad (2)$$

Q_{aux} in eqn (2) is the actual auxiliary energy required by the hybrid building.

To account for deadband settings in the active and auxiliary system controllers, the assumption is made that when either system is operating, the average indoor temperature is equal to the respective lower set point plus one half of the controller deadband. Simulation results have shown this assumption to be valid on a monthly-average basis[12]. The average indoor temperatures are defined in eqns (3) and (4) for the auxiliary and active solar systems.

$$\bar{T}_{aux} = T_{set,aux} + 1/2(\text{deadband})_{aux}, \quad (3)$$

$$\bar{T}_{act} = T_{set,act} + 1/2(\text{deadband})_{act}. \quad (4)$$

L, the actual load on the active system, can be determined by calculating the load on the active system as predicted by the passive design method, L_0, and adding the increase in active system load due to controller effects. L_o can be expressed on a UA degree–day basis:

$$L_o = UA_b(DD)(1 - f_p). \quad (5)$$

The increase in the active system load due to controller effect, $L - L_o$, must be expressed in terms of the total building energy loss coefficient (the building shell energy loss coefficient plus the passive collector energy loss coefficient) as there will be increased losses from both the building shell and the passive collector.

$$L - L_o = (UA_b + UA_c)(\bar{T}_{act} - \bar{T}_{aux})f_a N, \quad (6)$$

where N is the number of days in the month. Equations (5) and (6) can be rearranged to yield

$$\frac{L}{L_o} = 1 + \frac{(UA_b + UA_c)(\bar{T}_{act} - \bar{T}_{aux})f_a N}{UA_b(DD)(1 - f_p)}. \quad (7)$$

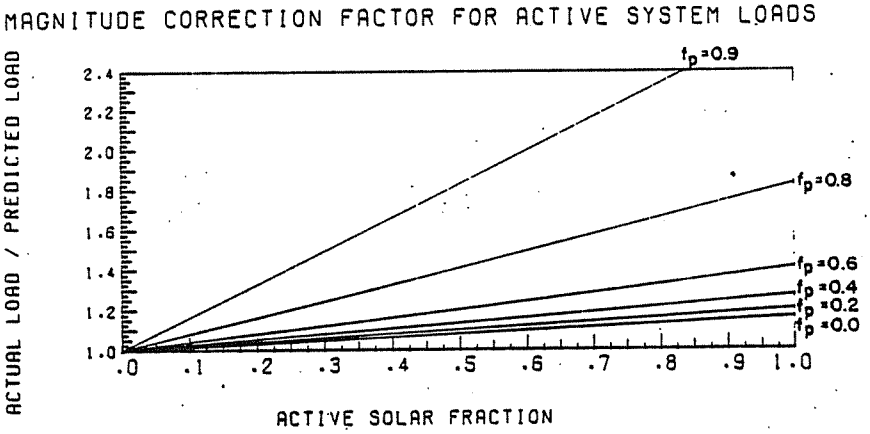

Fig. 1. Load magnitude correction factor for active systems loads. This plot is for N = 31 days, DD = 403 C-days T_{aux} = 18.5C, T_{act} = 20.0C and $(UA_B + UA_c)/UA_B$ = 1.5.

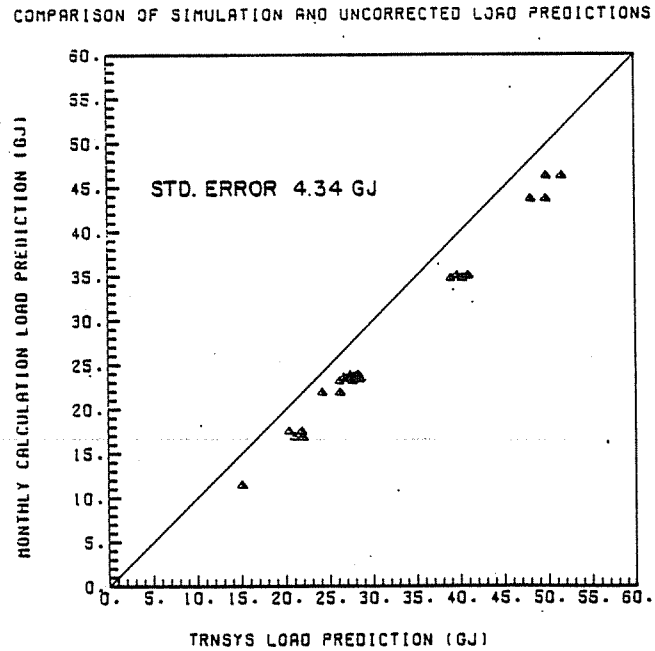

Fig. 2. Uncorrected annual active system loads compared to TRNSYS simulation results. The points are for Caribou, ME, Bismarck, ND, Columbia, MO, and New York, NY.

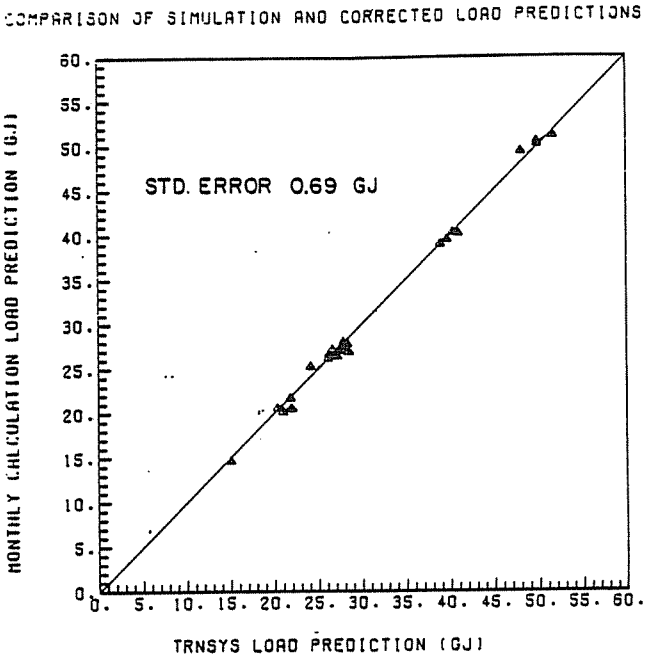

Fig. 3. Corrected annual active system loads compared to TRNSYS simulation results. The locations are the same as in Fig. 2.

Equation (7) indicates that if $f_a = 0$ (i.e. no active system), then L, the energy required in addition to the passive contribution to maintain the building at the set point temperature, is equal to L_o, the estimate provided by the passive system design method. As f_a is increased, the fraction of L provided by the active solar energy system, is increased, and L/L_o becomes greater than 1 as shown in Fig. 1. This figure is for a typical situation in which $N = 31$, $DD = 403$ C-days, $(UA_b + UA_c)/UA_b = 1.5$, $\bar{T}_{aux} = 18.5\ C$, and $\bar{T}_{act} = 20.0\ C$. For example, a passive solar fraction of 0.4, and high active solar fractions can result in loads which are 25% greater than those calculated based on the auxiliary set point temperature. This correction factor can (and should) be applied to active-only space heating systems (i.e. $f_p = 0$) as well, if the load estimates used in the design method calculations do not include the effect of elevated temperature resulting from controller settings, as is usually the case.

Table 1. Simulation and f-Chart parameters

Locations	
Seattle, WA	
Madison, WI	
Albuquerque, NM	
Boston, MA	
Passive components	
Direct gain	0.12m Collector
Storage Wall	0.25m Collector-storage wall
$U_{Collector}$: Day	2.5 W/°C m²
$U_{Collector}$: Night	1.5 W/°C m²
Collector Area	5–100 m²
Active components	
$F_R(\tau\alpha)$	0.7
$F_R U_L$	4.72 W/m²°C
Collector area	0–200 m²
Storage capacity	37–75l/m²
$\epsilon C_{min}/UA_b$	1.1–5.0
Building	
UA (without passive collector)	60–200 W/°C
Capacitance	2000–35000 kJ/°C
Auxiliary set temperature	18°C
Active set temperature	19°C
Deadbands	2°C
Allowable passive swing	4–8°C

The use of eqn (7) requires an iterative calculation procedure. The monthly passive solar fractions (f_p) are calculated from a passive design method. The net loads obtained from the passive method, L_o, are used in the f-Chart method to obtain monthly active solar fractions estimates. The monthly active solar fractions and the monthly degree–days are then used to find correction factors from eqn (7) which can be multiplied by monthly values of L_o to obtain better estimates of the monthly loads. The f-Chart calculations are then repeated. One iteration is generally all that is needed.

Figure 2 shows predicted annual active system loads that have not been corrected for controller effects compared to detailed simulation results for four locations. Figure 3 shows a similar comparison, except that the predicted active system loads have been corrected by use of the correction factor given in eqn (7). (In both of these plots, simulation results using the parameters shown in Table 1 were used to obtain the predicted active system loads, thereby eliminating any error that is associated with the simplified passive design methods.) Comparison of the two plots shows that eqn (7) corrects the active system load for controller effects to within a standard deviation of ±2% on an annual basis for all locations examined. Somewhat more error is associated with monthly calculations which were summed to get the annual values.

5. CORRECTION FACTOR FOR ACTIVE SYSTEM LOAD TIME DISTRIBUTION

The time distribution of the load on an active system is affected by the passive solar contribution. In a combined active–direct gain system, for example, the load on the active system will be shifted more toward nighttime, causing the active system to store energy for longer periods.

Storing energy raises the average collector inlet temperature and thereby reduces the efficiency of the active system. Design methods such as f-Chart do not account for this effect. Comparisons of detailed TRNSYS simulations of hybrid systems and design method predictions were used to develop an empirical correction factor for the time distribution effect. The parameters used in the simulations and f-Chart calculations are listed in Table 1. The f-Chart calculations were done using the computer program F-CHART 3.0[3], not to be confused with the ϕ, f-Chart method[4] used in F-CHART 4.1[5].

Before evaluating active–passive interactions it was first necessary to verify the accuracy of the f-Chart method for active systems alone, and to determine if there was any systematic bias which could mask the hybrid system interactions. As seen in Fig. 4, each of the four cities has a certain bias curve, with the difference in annual solar fractions between f-Chart predictions and TRNSYS calculations defined as (ΔF_a) being plotted as a function of annual solar fraction. Taken as a whole, the accuracy of f-Chart relative to TRNSYS appears to be $\pm 3\%$, as originally cited for the method[2]. The one exception to this is Seattle, WA, a location for which f-Chart has been previously shown[6] to underpredict due to the fact that the relatively small amount of sunshine in winter has a high utilizability. The more detailed calculations required by the ϕ, f-Chart method (i.e. F-CHART 4.1) should agree more closely with simulation results for Seattle.

A further study was conducted to determine the effect of building capacitance on active solar fraction predictions. Figure 5 shows a comparison of ΔF_a as a function of annual solar fraction and effective building capacitance. The heating systems control strategy used in these simulations is as follows. If the building temperature drops below 19°C, energy from the solar storage (if available) is added to the house; if the temperature continues to drop, the auxiliary furnace is turned on at 18°C. Both solar and auxiliary thermostats have 2°C deadbands. This control strategy is called temperature level control. Also shown in Fig. 5 are simulation results using energy rate control, the control strategy used in the development of the f-Charts. With energy rate control, the exact amount of energy needed during a given timestep is added to the building. This corresponds to a 0°C deadband controller, keeping the indoor air temperature constant. The product of the deadband and the building capacitance is a measure of the amount of energy which can be stored in the building mass. Temperature level control therefore allows additional energy storage. Figure 5 shows that the building capacitance does have a systematic effect on f-Chart calculations. However, between the extremes of 2000 kJ/°C to 35,000 kJ/°C, which would encompass buildings of very light to heavy construction, there is a maximum variation in ΔF_a of only 2.5%.

A final comparison between TRNSYS and F-CHART for active systems shows the effect of the active system load heat exchanger size. In the f-Chart method, load heat exchanger size is represented by the dimensionless parameter, $\epsilon C_{min}/UA_b$, where ϵ is the heat exchanger effectiveness, C_{min} is the minimum capacitance rate of the heat exchanger, and UA_b is the total building energy loss coefficient. A standard value of 2.0 for this parameter was used to develop the f-Charts for liquid-based systems, and non-standard values require a correction factor to the f-Chart dimensionless parameter, Y. Changes in $\epsilon C_{min}/UA_b$ produce a small distortion of the basic f-Chart accuracy for a reasonable range of values (1.1–5.0), with the only notable variation (about 3%) being in the 70%–90% solar fraction range.

The previous F-CHART–TRNSYS comparisons and the comparisons of hybrid systems to follow, are all based on monthly loads in F-CHART as calculated by the cor-

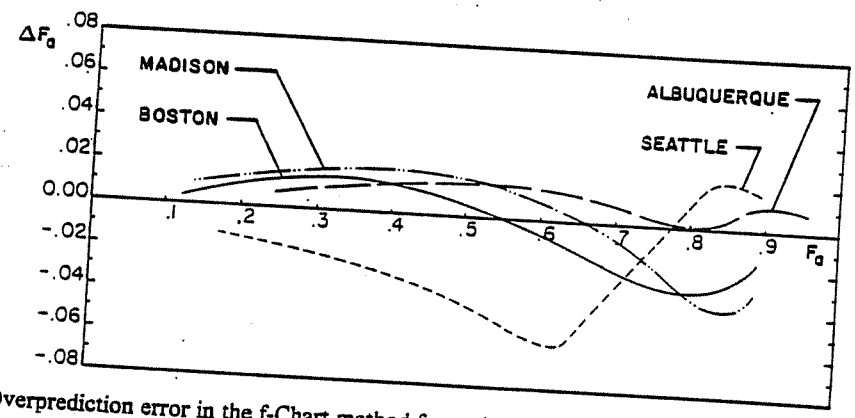

Fig. 4. Overprediction error in the f-Chart method for active only systems for different locations. All other parameters were constant.

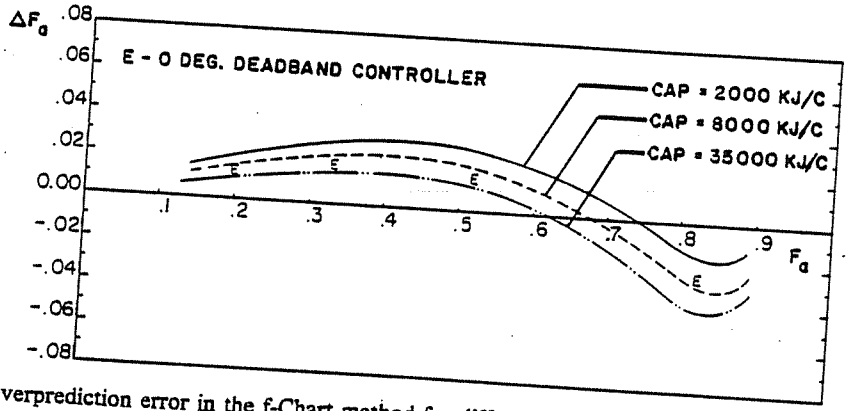

Fig. 5. Overprediction error in the f-Chart method for different building capacitances for an active-only system in Madison, WI.

responding TRNSYS simulations rather than load estimates obtained from a passive design method and eqn (7). This is done so that possible errors from these sources are not introduced into the time distribution correction factor derived from these comparisons.

The study of the use of the f-Chart method for estimating the active solar fraction in hybrid systems was based on TRNSYS simulations using the parameter values in Table 1. Comparisons of results from the simulations and f-Chart predictions were done in a manner similar to the previous studies, i.e. by plotting ΔF_a as a function of active solar fraction. The major difference was that the f-Chart bias for active systems alone was subtracted out so that the effect of hybrid interaction could be plotted independently. Following this procedure, it was found that building capacitance has little effect on hybrid interaction on a yearly basis; or in other words, the effect of building capacitance on f-Chart predictions of hybrid system performance was no more pronounced than it was for active systems alone. Similarly, the effect of $\epsilon C_{min}/UA_b$ was found to have minimal effect.

Based on these results, the important parameters in hybrid systems are: active solar fraction, passive solar fraction, and active system storage capacity relative to collector size. A range of active and passive solar fractions (0%–90% for active, 0%–60% for passive) were studied by varying their respective collector areas. Active system storage was investigated for the f-Chart standard storage (314 kJ/°Cm^2) and for one-half of the standard storage (157 kJ/°Cm^2). Different passive gain time distributions were studied using direct-gain, 0.25 m concrete collector-storage wall, and 0.125 m concrete collector-storage wall systems.

The change in the active system load distribution will always be greater for direct-gain systems than for collector-storage walls. The direct-gain meets the load during the day, causing the active system to store energy during the day, thereby raising the storage tank or pebble bed temperature more than it normally would be raised if a direct-gain system were not involved. This, in turn, raises the collector inlet temperature, and reduces the collector efficiency. Collector-storage walls moderate the effect somewhat by delaying passive gains toward the evening, allowing some of the energy collected by the active system during the day to be used immediately, thereby lowering the average storage temperature and more closely resembling the load distribution assumed by the f-Chart method. Because direct-gain is the limiting case of hybrid interaction, and because the overall error in f-Chart predictions of active solar fractions in hybrid systems is relatively small, results of the direct-gain hybrid systems will be presented as the upper bound of f-Chart overpredictions for hybrid systems. These results can be used directly to obtain a time distribution correction factor for active performance in direct-gain hybrid systems calculated by the f-Chart method and will provide a slightly conservative estimate for collector-storage wall hybrid systems. Figures 6 and 7 show plots of the f-Chart time distribution correction factor (ΔF_a) derived from TRNSYS simulations as a function of annual active solar fraction (F_a) and annual

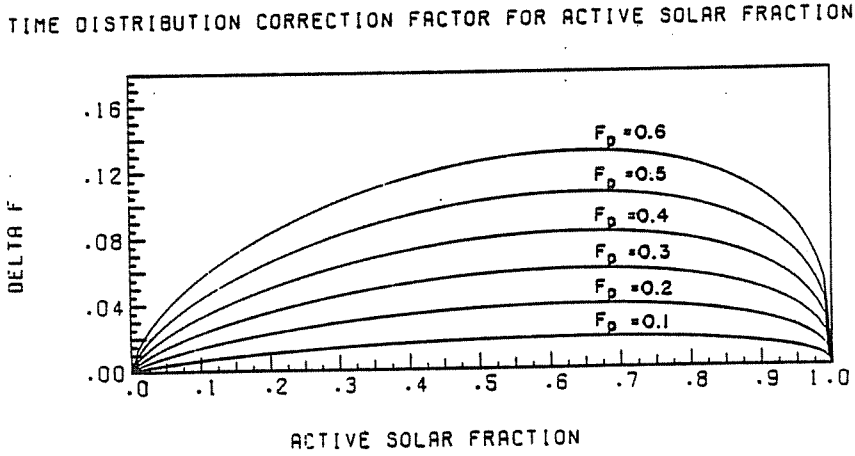

Fig. 6. Active system load time distribution correction factor for an active system storage capacity of 157 KJ/Cm^2.

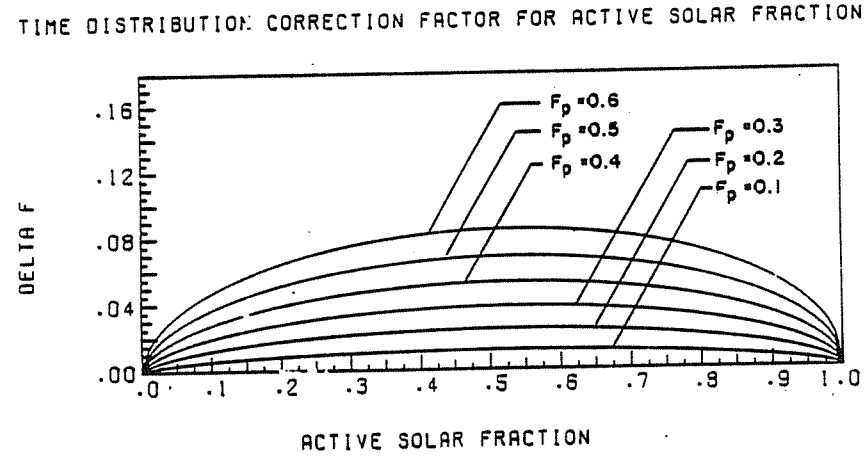

Fig. 7. Active system load time distribution correction factor for an active system storage capacity of 314 KJ/Cm^2.

passive solar fraction (F_p) for active storage capacities of 314 and 157 kJ/°Cm², respectively.

The time distribution correction factor is presented on an annual rather than monthly basis because it provides a slightly better estimate of the auxiliary energy requirement if applied on an annual basis. As presented, the correction factor should not be applied on a monthly basis as the monthly passive solar fraction could exceed the limits of the correction factor correlation ($F_p \leq 0.6$). (If a monthly auxiliary estimate is necessary, the annual value of ΔF_a can be applied to the monthly active solar fractions to obtain approximate monthly auxiliary values. This does not give a strictly correct monthly distribution of auxiliary energy use, but the error appears to be less than the random error inherent in the f-Chart method.)

The error in f-Chart predictions is larger for higher passive fractions and for smaller active storage capacities. This would be expected because both of these conditions would accentuate the problems associated with raising the active storage temperature during the day. The fact that the f-Chart prediction approaches the TRNSYS calculations at active solar fractions 0% and 100% can also be

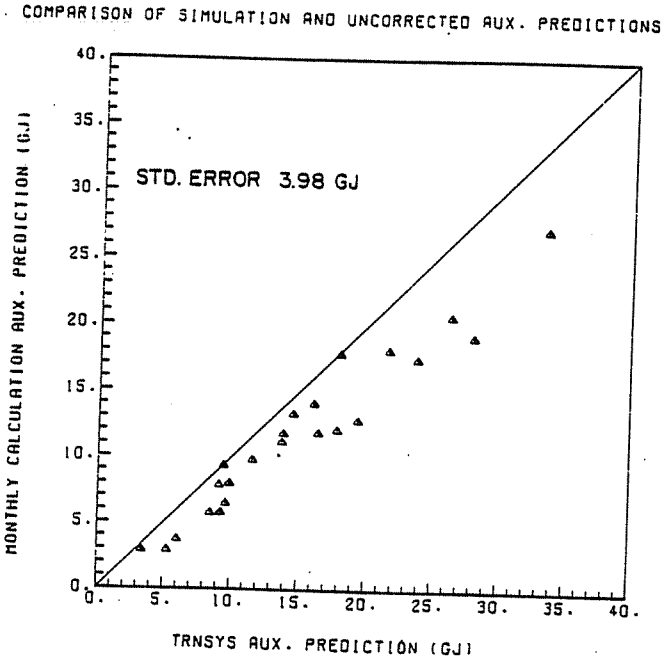

Fig. 8. Uncorrected design method predictions of auxiliary energy use compared to TRNSYS simulation results. The locations are Caribou, ME, Bismarck, ND, Columbia, MO, and New York, NY.

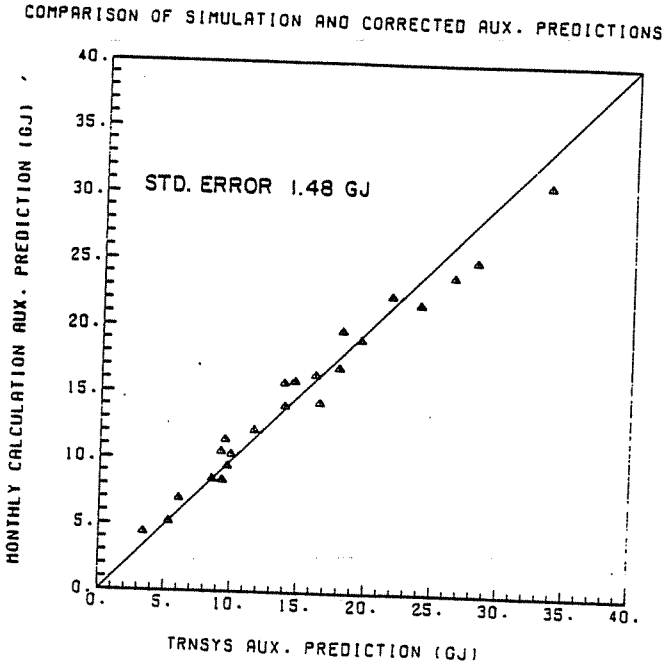

Fig. 9. Design method predictions of auxiliary energy use using the active system load magnitude and time distribution correction factors compared to TRNSYS simulation results. The locations are the same as in Fig. 8.

Table 2. Values of constants appearing in eqn. (8)

	Active Storage Capacity	
	314 kJ/°Cm²	157 kJ/°Cm²
C_1 =	0.287	0.410
C_2 =	0.246	0.285
C_3 =	0.216	0.154

deduced. At F_a equal to 0%, there is no interaction effect, and the correction factor should be zero. At 100% active solar fraction, the active system is so large relative to the load, it supplies all of the necessary energy regardless of the minor interactions with the passive system.

The time distribution correction factor for collector-storage walls always had values less than the corresponding direct-gain values, but they could not be correlated because the effect of location was of the same magnitude as the f-Chart overprediction.

Curve fits for the information in Figs. 6 and 7 are:

$$\Delta F_a = C_1 \cdot F_a^{C_2(2.8-F_p)} \cdot (1 - F_a)^{C_3(2.8-F_p)} \cdot F_p, \quad (8)$$

where C_1, C_2, and C_3 depend on active storage capacity as indicated in Table 2. This correction factor should be applied on an annual basis to the active solar fraction predicted by the f-Chart method, lowering the uncorrected solar fraction F_a to the value F'_a as defined in eqn (9).

$$F'_a = F_a - \Delta F_a. \quad (9)$$

The time distribution correction factor should be used in conjunction with the load magnitude correction factor described previously as they are of similar magnitudes. Figures 8 and 9 show a comparison of design method and simulation predictions of auxiliary energy use with and without the two hybrid correction factors for 23 examples in Bismark, ND, Caribou ME, Columbia, MO and New York, NY. For these plots, the SLR method[7] was used for the passive system analysis. The average of the absolute value of the bias error for the uncorrected predictions was 22%. When the load magnitude and time distribution correction factors were applied, the error was reduced to about 8%. Further reductions in the average error are unlikely, since a large portion of this remaining error is inherent in the passive and active design methods.

6. SUMMARY

A study of hybrid space heating systems has found that there are two major sources of systematic error associated with using existing design methods successively on the passive and active subsystems. The first is associated with the effects of the active system controller which increases the load on the active system as a function of controller parameters, active solar fraction and passive solar fraction. An analytical equation has been developed to correct the active system load predicted by a passive design method for the controller effects.

The second systematic error is caused by the effect of the passive system on the time distribution of the active system load. An empirical correction factor for the f-Chart method has been developed to account for the effect of load distribution in a combined direct-gain active hybrid system. In all cases, direct-gain passive systems will cause more interference than collector-storage wall systems with the active system in a way in which the f-Chart method cannot predict. This interaction occurs because the direct-gain competes directly with the active system during the day, resulting in higher collector inlet temperatures, and therefore, lower collector efficiency. Collector-storage walls, on the other hand, offset the passive gains somewhat. The thicker the wall, the more the gains will be distributed and will more closely resemble a distributed load, thereby having less effect upon the active system. The time distribution correction factor will therefore give a conservative estimate of the active system performance in collector-storage wall hybrid systems.

In all cases, the error in the f-Chart method is relatively small and may be overshadowed by other uncertainties. Errors in such factors as passive system design calculations, load calculations, building capacitance, and meteorological data can give errors of a similar or larger magnitude.

7. EXAMPLE

As an example of the use of the active system load and solar fraction correction factors, a direct-gain hybrid system located in Madison, WI will be analyzed. System parameters and meteorological data for January are given in Table 3.

Tilted surface radiation for both the active and passive systems was calculated using the method in Klein and Theilacker[10], with the monthly diffuse fraction estimated using the correlation developed by Erbs *et al.*[11]. The passive calculations were done using the Un-utilizability method[8] and are summarized in Table 4. The last column in Table 4 shows corresponding values from a TRNSYS simulation, giving an idea of the error associated with the passive design method for this system.

From these calculations, the active system load for zero collector area (L_o) for January is 10.55 GJ. This value is used as a first approximation of the net load in the active system (L). Using the f-Chart method, the active solar fraction for January is found to be:

$$f_a = 0.444.$$

The estimated auxiliary from January is

$$\text{Aux} = (1 - f_a)(L_o) = 5.87 \text{ GJ}.$$

Equation (7) is now used to correct the estimated load with

$$DD = 819°\text{C-days}; \; f_p = 0.001; \; f_a = 0.444,$$

Table 3. Example problem parameters

Location: Madison, WI; Lat: 431°	
System Data	
Passive Components	
Collector area (direct gain)	40 m²
U_{window}: Day	2.5 W/°C m²
U_{window}: Night	1.5 W/°C m²
$(\overline{\tau\alpha})$	0.7
Active Components	
Collector area (β = 60, γ = 0)	40 m²
F_R $(\tau\alpha)$	0.7
$F_R(U_L)$	4.72 W/°C m²
Storage capacity (water)	75 l/m²
Building	
UA (without passive window)	150 W/°C
Capacitance	17000 kJ/°C
Auxiliary set temperature	18°C
Active set temperature	19°C
Deadbands	2°C
Allowable passive swing temperature	8°C
January Data	
DD = 819 °C-days	
$\overline{H}_{hor}$ = 5877 kJ/m²-day	

Table 4. Passive analysis (un-utilizability method)

	Building losses	Window losses	L_o	Solar fraction	TRNSYS L_o
J	10.61 GJ	5.66 GJ	10.60	0.001	9.91
F	8.70	4.64	7.66	0.120	7.19
M	7.98	4.26	5.85	0.267	6.03
A	3.73	1.99	1.73	0.464	2.10
M	1.94	1.04	0.02	0.990	0.76
S	1.13	0.61	0.00	1.00	0.16
O	6.08	3.25	5.22	0.142	5.48
N	8.73	4.65	9.13	−0.050	9.19
D	52.03	27.77	41.41	.204	42.59

and the controller settings shown in Table 3,

$$\frac{L}{L_o} = 1.039,$$

$$L = 1.039(10.60) = 11.01 \text{ GJ}.$$

The new value of L is then used to repeat the f-Chart calculations to obtain a more accurate monthly auxiliary load. Using this load, the f-Chart method gives

$$f_a = 0.405,$$

$$Q_{aux} = (1 - 0.405)(11.00) = 6.55 \text{ GJ}.$$

A summary of the results for the nine heating-season months is shown in Table 5. The time distribution correction factor can then be applied to the annual active solar fraction. Using the annual passive solar fraction, $F_p = 0.204$, and the annual active solar fraction $F_a = 0.582$, eqn (8) gives an F value of 0.025. The actual active solar fraction F'_a can then be found

$$F'_a = 0.582 - 0.025 = 0.557.$$

This gives an annual auxiliary energy use of

$$Q_{aux} = (1 - 0.557)46.62 = 20.65 \text{ GJ}.$$

Table 6 shows the design method results for active system loads and auxiliary energy, compared to detailed TRNSYS simulation results. On an annual basis, the design method active system load for this example is within 1.2% of the simulation results. The predicted annual auxiliary is within 1% of the simulation results.

Table 5. Active analysis (f-Chart) method

	First approximation			Second approximation	
	f_a	DD	L/L_o	L	f_a
J	0.444	819	1.039	11.01	0.405
F	0.676	672	1.074	8.22	0.634
M	0.878	616	1.139	6.66	0.923
A	1.0	288	1.447	2.50	1.0
M	1.0	150	48.55	0.97	1.0
S	1.0	87	—	0.0	—
N	0.581	469	1.100	5.74	0.588
D	0.304	673	1.031	9.41	0.253
	0.583			46.62	0.582

Table 6. Comparison of design method and simulation results

	Design method		TRNSYS simulation	
	L	Q_{aux}	L	Q_{aux}
J	11.01 GJ	6.55 GJ	10.18 GJ	6.59 GJ
F	8.22	3.01	7.68	3.46
M	6.66	.51	6.98	1.05
A	2.50	0.00	2.85	0.04
M	0.97	0.00	1.15	0.06
S	0.0	0.00	0.33	0.0
O	2.11	0.00	2.59	0.0
N	5.74	2.36	6.01	2.79
D	9.41	7.03	9.39	6.73
	46.52	19.46	47.15	20.71
		(20.65)		

* Modified for the load time distribution, the predicted auxiliary energy requirement is 20.65 GJ.

REFERENCES

1. TRNSYS 11.1, EES Report 38, University of Wisconsin-Madison (1981).
2. S. A. Klein et al., A design procedure for solar heating systems. *Solar Energy* **18**, 113 (1976).
3. F-CHART 3.0, EES Report 49, University of Wisconsin-Madison (1978).
4. S. A. Klein and W. A. Beckman, A generalized design method for closed-loop solar energy systems. *Solar Energy* **22**, 269 (1979).
5. F-CHART 4.1, EES Report 50, University of Wisconsin-Madison (1980).
6. J. A. Duffie and W. A. Beckman, *Solar Engineering of Thermal Processes*. Wiley-Interscience, New York (1980).
7. J. D. Balcomb, et al., Expanding the SLR method. *Passive Solar Journal* **1**, 67 (1982).
8. W. A. Monsen, et al., Prediction of direct gain solar heating system performance. *Solar Energy* **27**, 143 (1981).
9. W. A. Monsen, et al., The un-utilizability method for collector storage walls. *Solar Energy* **29**, 421 (1982).
10. S. A. Klein and J. C. Theilacker, An algorithm for calculating monthly-average radiation on inclined surfaces. *ASME Journal of Solar Energy Engineering* **103**, 29 (1981).
11. D. G. Erbs, *et al.*, Estimation of the diffuse radiation fraction for hourly, daily, and monthly-average global radiation. *Solar energy* **28**(4), 293 (1982).
12. B. D. Evans, Design methods for active–passive hybrid space heating systems. M.S. Thesis, University of Wisconsin-Madison (1983).
13. R. W. Jones, (ed.); J. D. Balcomb, et al., *Passive Solar Design Handbook*. **3**, U.S. Dept. of Energy, DOE/CS-0127/3 (1982).